# Multichannel combining and equalization for underwater acoustic MIMO channels

Aijun Song and Mohsen Badiey
College of Marine and Earth Studies
University of Delaware
Newark, DE 19716 USA

Vincent K. McDonald
Space and Naval Warfare Systems Center
San Diego, CA 92152 USA

***Abstract*—In order to achieve high data rate digital communications, multiple-input/multiple-output (MIMO) techniques have attracted growing interests in the underwater acoustic communication studies. In this paper, multichannel combining and decision feedback equalization (MCC/DFE) has been proposed for underwater acoustic MIMO channels. In order to overcome the difficulties introduced by the fast fluctuating channel, Doppler tracking and frequent channel estimation are performed. Then time reversal combining followed by a single channel DFE is used to demodulate individual symbol sequences transmitted by the multiple element source. To improve the performance, successive interference cancellation is also incorporated into the receiver structure.**

**Using data from the Makai experiment conducted around Kauai Island, HI, 2005, we have shown that the achievable data rate can be increased up to 4 times using the same bandwidth as single source systems. For example, 32 kilobits/s could have been achieved by simultaneous transmission of four 4 kilosymbols/s 4-phase shift keying (QPSK) symbol sequences when both the source and the receiver were drifting at a 2 km range in the ocean.**

## I. Introduction

Underwater acoustic communications can provide a flexible and cost-effective way to exchange information between underwater platforms. However, high data rate underwater acoustic communications is challenging because of severe multi-path spread, time varying property and limited bandwidth of the channel [1]. As being bandwidth efficient in a rich scattering environment [2]–[4], multiple-input/multiple-output (MIMO) techniques have attracted growing interests in the underwater acoustic communication studies. Based on the multichannel DFE structure proposed by Stojanovic *et al* [5]–[7], various receivers for MIMO systems were developed with a focus on the utilization of error correcting codes [8]–[10]. In [11]–[13], the time reversal based MIMO receivers were developed by taking advantage of spatial diversity of underwater acoustic channels.

In this paper, a multichannel combining and decision feedback equalizer (MCC/DFE) has been proposed for underwater acoustic MIMO channels based on the receiver for single source systems presented in [14]. Using data obtained from the Makai experiment (MakaiEx) [15], [16] conducted around Kauai Island, HI, 2005, we have shown that the achievable data rate can be increased 2 to 4 times using the same bandwidth as single source systems. In Section II, the MIMO system model is briefly presented. The receiver structure is presented in Section III. The experimental results are shown in Section IV. In the following sections, a variable with $\hat{}$ denotes the estimate of the variable. $c^*$ denotes the complex conjugate of a complex number $c$. $a(n)*b(n)$ denotes the convolution of two sequences $a(n)$ and $b(n)$.

## II. System Model

Consider an underwater acoustic MIMO system with $N_T$ transducers and $N_R$ hydrophones. At the $l$-th transducer at the source, an information symbol sequence $x_l(n)$ is modulated to carrier frequency $f_c$ and transmitted. All $N_T$ symbol sequences from $N_T$ transducers are independent of each other but with the same symbol rate $R$ and carrier frequency $f_c$. Let $y_m(t)$ be the received baseband signal at the $m$-th hydrophone. The effect of the transmission medium between the $l$-th transducer and the $m$-th hydrophone can be characterized by a time-varying channel impulse response (CIR) function, $h_{l,m}(t,\tau)$. Then the received signal on the $m$-th hydrophone $y_m(t)$ is the summation of all symbol sequences distorted by the channel. The analog waveform $y_m(t)$ is sampled at a fractional symbol interval to provide robustness to carrier phase fluctuations in the underwater acoustic channel [5], [17]. However, for notation convenience, symbol spaced signals are used throughout the paper. Then,

$$y_m(n) = \sum_{l=1}^{N_T} e^{j\theta_{l,m}(n)} \left[x_l(n) * h_{l,m}(n,\mu)\right] + v_m(n), \quad (1)$$

where $y_m(n)$ is the discrete time representation of the analog signal $y_m(t)$, $\theta_{l,m}(n)$ is the instantaneous carrier phase offset associated with the $l$-th symbol sequence, and $v_m(n)$ represents the ambient noise. $h_{l,m}(n,\mu)$, $0 \le \mu \le L-1$, is the discrete time baseband CIR function where $L$ is the duration in symbols for all the channels. $h_{l,m}(n,\mu)$ includes the combined effects of transmitter/receiver filters and the CIR function.

The challenge in underwater acoustic communications mainly lies in the highly dispersive and time varying characteristics of the channel. At high data rate coherent communications, the length channel $L$ is usually more than tens of symbols. Further, multiple hydrophones are employed to achieve desired performance for even single source underwater

978-1-4244-2620-1/08/$25.00 ©2008 IEEE

# Report Documentation Page

*Form Approved*
*OMB No. 0704-0188*



| 1. REPORT DATE | 2. REPORT TYPE | 3. DATES COVERED |
|---|---|---|
| **SEP 2008** | | **00-00-2008 to 00-00-2008** |

| 4. TITLE AND SUBTITLE | 5a. CONTRACT NUMBER |
|---|---|
| **Multichannel combining and equalization for underwater acoustic MIMO channels** | 5b. GRANT NUMBER |
| | 5c. PROGRAM ELEMENT NUMBER |
| 6. AUTHOR(S) | 5d. PROJECT NUMBER |
| | 5e. TASK NUMBER |
| | 5f. WORK UNIT NUMBER |
| 7. PERFORMING ORGANIZATION NAME(S) AND ADDRESS(ES) **Space and Naval Warfare Systems Center,San Diego,CA,92152** | 8. PERFORMING ORGANIZATION REPORT NUMBER |
| 9. SPONSORING/MONITORING AGENCY NAME(S) AND ADDRESS(ES) | 10. SPONSOR/MONITOR'S ACRONYM(S) |
| | 11. SPONSOR/MONITOR'S REPORT NUMBER(S) |

12. DISTRIBUTION/AVAILABILITY STATEMENT
**Approved for public release; distribution unlimited**

13. SUPPLEMENTARY NOTES
**See also ADM002176. Presented at the MTS/IEEE Oceans 2008 Conference and Exhibition held in Quebec City, Canada on 15-18 September 2008.**

14. ABSTRACT
**see report**

15. SUBJECT TERMS

| 16. SECURITY CLASSIFICATION OF: | | | 17. LIMITATION OF ABSTRACT | 18. NUMBER OF PAGES | 19a. NAME OF RESPONSIBLE PERSON |
|---|---|---|---|---|---|
| a. REPORT **unclassified** | b. ABSTRACT **unclassified** | c. THIS PAGE **unclassified** | **Same as Report (SAR)** | **6** | |

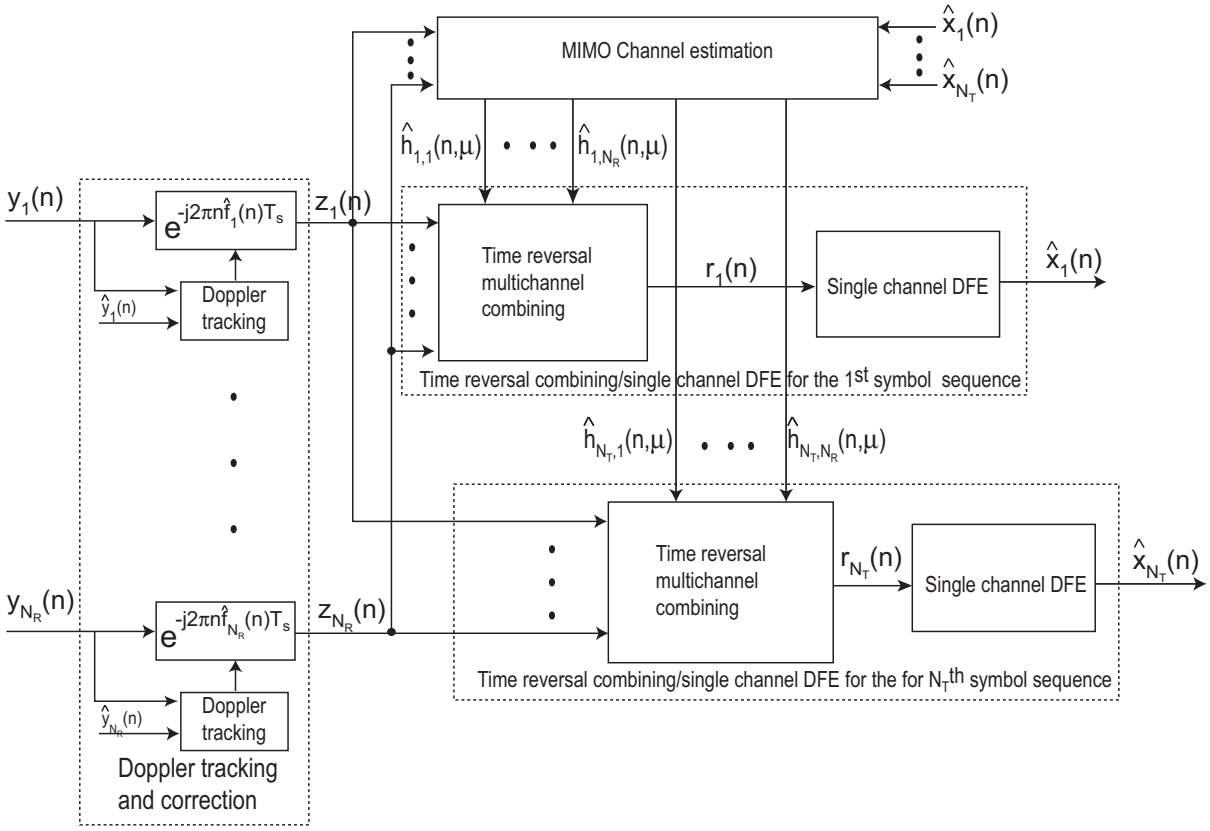


Fig. 1. The MCC/DFE structure for MIMO systems.

systems. Therefore, the implementation complexity should be taken into account in the design to deal with multiple highly dispersive channels.

## III. Receiver Structure

In this section, a low complexity MCC/DFE structure for underwater acoustic MIMO systems is proposed based on the receiver in [14]. The MCC/DFE combined with successive interference cancellation (SIC) [17] is also presented.

### A. The MCC/DFE structure

As shown in Fig. 1, the receiver consists of three components: Doppler tracking and correction, MIMO channel estimation, and time reversal combining and single channel DFE. Doppler tracking and correction is used to compensate for Doppler shift and any other linear trend in the carrier phase offset. MIMO channel estimation is performed based on the Doppler corrected signals and multiple estimated symbol sequences. To demodulate the $l$-th symbol sequence, time reversal combining and single channel DFE are followed.

The proposed receiver is a channel estimation based structure. At the beginning of a data packet, a preamble, or a sequence of known symbols, is used to perform initial channel and Doppler estimation and to train adaptively the DFE tap weights. After the preamble, channel and Doppler estimation are frequently updated. The most recent channel estimate is denoted by $\hat{h}_{l,m}(n,\mu)$ and the most recent Doppler estimate is denoted by $\hat{f}_m(n)$. The major parts of the receiver now will be discussed.

*1) Doppler tracking and correction:* The Doppler estimate at the $m$-th hydrophone is obtained by

$$\hat{f}_m(n) = \arg\max_f \left| \sum_{p=0}^{N_\Delta - 1} y_m(n-p)(\hat{y}_m(n-p)e^{j2\pi p f Ts})^* \right|, \tag{2}$$

where $\hat{y}_m(n) = \sum_{l=1}^{N_T} \hat{x}_l(n) * \hat{h}_{l,m}(n,\mu)$ and $T_s = 1/R$ is the symbol duration. In Eq. 2, $N_\Delta$ is the Doppler observation block size in symbols and $f_m^0 - \frac{1}{2}\delta f < f < f_m^0 + \frac{1}{2}\delta f$, where $f_m^0$ is the coarse Doppler estimate and $\delta f$ is the Doppler search range. Since Doppler is estimated frequently, $f_m^0$ is set to the previous Doppler estimate. The Doppler correction is performed by offsetting the received signal $y_m(n)$ by the estimated Doppler shift, i.e., $z_m(n) = y_m(n)e^{-j2\pi n \hat{f}_m(n) T_s}$, where $z_m(n)$ denotes the Doppler corrected signal.

*2) MIMO Channel estimation:* Assuming carrier phase offset $\theta_{l,m}(n)$ can be removed completely by the Doppler correction, we have

$$z_m(n) = \sum_{l=1}^{N_T} x_l(n) * h_{l,m}(n,\mu) + v'_m(n), \tag{3}$$

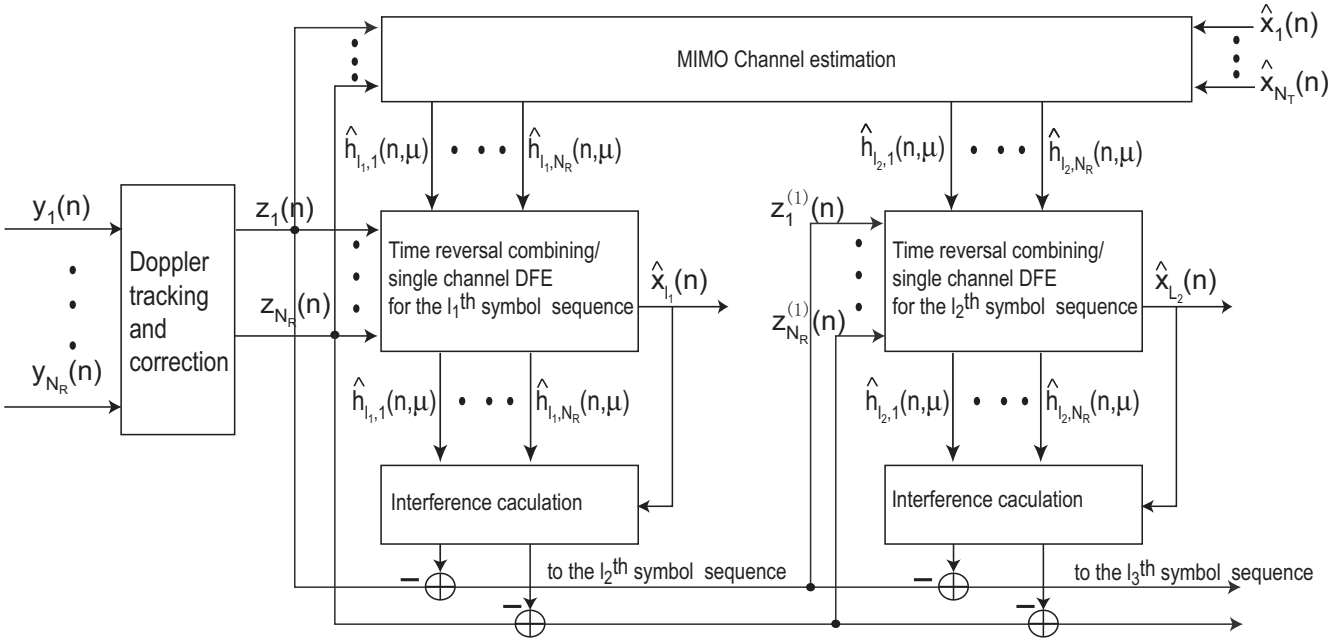


Fig. 2. The MCC/DFE structure with SIC.

where $v'_m(n)$ is the noise term after Doppler correction. The $N_T N_R$ channel estimates $\hat{h}_{l,m}(n,\mu)$ can be obtained jointly based on the Doppler corrected signal $z_m(n)$ and the previously detected symbols $\hat{x}_l(n)$ or the known symbols $x_l(n)$. Various least squares algorithms can be used for channel estimation. In this paper, the iterative least squares QR (LSQR) algorithm is used [18]. The channel estimation block size is chosen to be three times the total channel taps to be estimated, i.e., $N_0 = 3N_T L$.

*3) Time reversal combining and single channel DFE for the $l$-th symbol sequence:* To demodulate the $l$-th symbol sequence, the other symbol sequences can be treated as noise. The time reversal combining and the single DFE can be used to demodulate individual symbol sequence.

Time reversal combining uses $(\hat{h}_{l,m}(n,-\mu))^*$ to match-filter the Doppler-corrected signals on each channel $z_m(n)$ and then combines the results [19]–[21]. The output of time reversal combining is

$$\begin{aligned} r_l(n) &= \sum_{m=1}^{N_R} (\hat{h}_{l,m}(n,-\mu))^* * z_m(n) \\ &= x_l(n) * q_l(n,\mu) + w_l(n), \end{aligned} \tag{4}$$

where $w_l(n)$ is the noise component,

$$w_l(n) = \sum_{m=1}^{N_R} (\hat{h}_{l,m}(n,-\mu))^* * (v'_m(n)), \tag{5}$$

and $q_l(n,l)$ is the effective CIR function, or the q-function [22], between the $l$-th transducer and the receiver:

$$q_l(n,l) = \sum_{m=1}^{N_R} (\hat{h}_{l,m}(n,-\mu))^* * h_{l,m}(n,\mu). \tag{6}$$

A single channel DFE with joint phase tracking [6] is used to equalize the residual inter-symbol interference in $r_l(n)$. The exponentially weighted recursive least-squares (RLS) algorithm is used to update the equalizer tap weights. The residual carrier phase offset in $r_l(n)$ is compensated for by a second order phase locked loop (PLL) embedded in the adaptive channel equalizer. The phase correction based on the PLL output is implemented at the input to the DFE feedforward filter. The soft output signal-to-noise ratio (SNR), $\rho$, of the single channel DFE is used as a performance metric in this paper.

### *B. The MCC/DFE structure with SIC*

In MIMO systems, multiple symbol sequences are simultaneously transmitted and each symbol sequence causes interference in the demodulation of other data streams. In other words, co-channel interference exists because multiple symbol sequences share the use of the same channel and frequency band. In order to mitigate the co-channel interference, SIC [17] can be incorporated into the MCC/DFE structure. The symbol sequences are demodulated in the order of the soft output SNR of the single channel DFE. As shown in Fig. 2, the strongest symbol sequence, the $l_1$-th symbol sequence, is to be demodulated first. After the $l_i$-th symbol sequence is demodulated, interference resulted from it will be removed. That is,

$$z_m^{(i)}(n) = z_m^{(i-1)}(n) - \hat{x}_{l_i}(n) * \hat{h}_{l_i,m}(n,\mu), \tag{7}$$

where $z_m^{(i)}(n)$ denotes the Doppler corrected signal with the interference removed from the strongest $i$ symbol sequences. Then the $l_{i+1}$-th symbol sequence is demodulated based on $z_m^{(i)}(n)$.

### C. Comparison with existing acoustic MIMO receivers

In the literature, existing acoustic MIMO receivers include: (1) multichannel DFE based MIMO receivers in [7]–[10] and (2) the time reversal MIMO receivers in [11]–[13]. In the multichannel DFE based MIMO receivers, feedforward filters are applied to the individual channels and their outputs are combined prior to the feedback filter as in the multichannel DFE [5]. Phase synchronization at the individual channels is optimized jointly with the equalizer tap weights. The number of adaptive feedforward taps increases with the number of hydrophones. Unlike the multichannel DFE based MIMO receivers, the proposed receiver uses a single channel DFE after time reversal combining for each symbol sequence.

An advantage of the proposed receiver structure is its low complexity. For the demodulation of each symbol sequence, the complexity of a multichannel DFE based MIMO receiver increases at least as the square of the number of hydrophones if RLS algorithms are used for a fast tracking capability [17]. Since time reversal combining collapses multiple channels into a single channel, the complexity of the successive DFE remains unchanged when the number of hydrophones increases.

Although also time reversal based, the proposed receiver has a different structure than the time reversal MIMO receiver in [11]–[13] where multichannel combining is performed based on channel probes or the known symbols at the beginning of the data packet. Phase tracking or Doppler tracking usually is performed after time reversal combining. Compared with the referenced time reversal MIMO receivers, the proposed receiver performs continuous Doppler tracking and channel estimation to overcome fast fluctuations which occur over the duration of a data packet.

## IV. Experimental Results

MakaiEx was conducted from Sept. 15 to Oct. 2, 2005, west of Kauai, HI, to study high-frequency underwater acoustic communicatons [15]. During MakaiEx, the 10 element verctical MIMO source provided by Space and Naval Warfare Systems Center and the 8 element ACDS receiving array provided by Naval Research Laboratory (NRL) were deployed three separate times [16]. In this paper, the data from the second MIMO deployment on Sept 26, 2005 will be analyzed. The 8 element ACDS receiving array was deployed by the R/V Kilo Moana and set in a free drift mode. The top element of the ACDS array was about 20 m below the sea surface and the spacing was about 2 m. The sampling frequency of the ACDS array was 160 kHz. The 10 element MIMO source was hang from the deck of the R/V Kilo Moana. The spacing of the source element was 2 m with the top element about 20 m below the sea surface. The source power level of each source element is 190 dB re 1 $\mu Pa$ at 1 m. Once deployed, the R/V Kilo Moana maintained roughly a 2 km separation with the ACDS array. The water depth of the experimental site was about 100 m.

The carrier frequency of the analyzed communication signal is $f_c = 37.5$ kHz and the symbol rate is $R = 4$ kilosymbols/s. The square-root raised cosine shaping filter is used with an excess bandwidth [17] of $75\%$. The communication data were in a form of packets. A 1248 symbol long preamble preceded the data packet. Then each 800 symbol data block was protected by a 224 symbol prefix and a 224 symbol appendix. The prefix and appendix were used to periodically retrain the equalizer. After the preamble, 7 data blocks were transmitted continuously. Note the 7-th block had a variable length less than 800 symbols. The total length of the packet was about 2.5 s. The data packet is illustrated in Fig. 3. Three types of source options were used, i.e., 1 transducer, 2 transducers, and 4 transducers, to transmit binary phase shift keying (BPSK) and 4 phase shift keying (QPSK) signals. A total of 6 packets are shown to demonstrate the receiver performance.

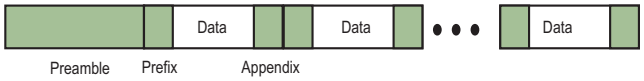


Fig. 3. The formation of the data packet.

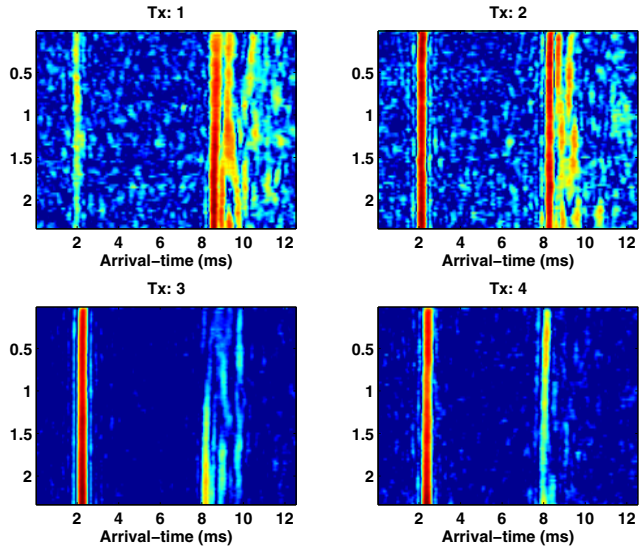


Fig. 4. The CIR function on the top receiving element of the ACDS array. The depths of the source elements are 22 m, 26 m, 32 m, and 38 m, respectively. Color scale has a 20 dB dynamic range.

As mentioned, fractional spaced sampling is used in the receiver and the oversampling rate is $K = 4$. The estimated length of the CIR function is 25 ms, or $L = 100$ symbols, for the single element source packets. It is set as $L = 50$ symbols for the multiple element source packets. The channel estimation block size $N_0$ and Doppler observation block size $N_\Delta$ are both set as $3N_TL$. The channel estimation update interval is chosen as $N = 100$ symbols. At the beginning of the packet, 1248 symbols are used to conduct initial channel estimation, Doppler tracking, and DFE tap weight training. The Doppler search range is $\delta f = 1.6$ Hz. The number of the feedforward taps is $KN_{ff} = 40$ symbols for the fractionally spaced DFE [6] where $N_{ff} = 10$ is the feedforward filter span in symbols. The number of the feedback taps is $N_{fb} = 2$

TABLE I
RECEIVER PARAMETERS.

| Parameters | Description | Value |
|---|---|---|
| $f_s$ | Sampling rate | 160 kHz |
| $f_c$ | Carrier frequency | 37.5 kHz |
| $R$ | Symbol rate | 4 kHz |
| $f_{EB}$ | Excess bandwidth of the square-root raised cosine filter | 3 kHz |
| $K$ | Oversampling factor | 4 |
| $N_R$ | Total number of the hydrophone channels | 8 |
| $N_{preamble}$ | Size of the preamble | 1000 symbols |
| $L$ | Length of the CIR function | 50 or 100 symbols |
| $N_0$ | Channel estimation block size | $2N_TL$ symbols |
| $N$ | Channel estimation update interval | 100 symbols |
| $N_\Delta$ | Doppler observation block size | $3N_TL$ symbols |
| $\delta f$ | Doppler search range | 1.6 Hz |
| $N_{ff}$ | Feedforward filter span in symbols | 10 symbols |
| $N_{fb}$ | Feedback filter tap number | 2 symbols |
| $K_{f_1}$ | Proportional tracking constant in PLL | 0.0002 |
| $K_{f_2}$ | Integral tracking constant in PLL | 0.0002 |
| $\lambda$ | RLS forgetting factor in the DFE | 0.999 |

because the feedback filter is applied to a symbol spaced sequence. The RLS forgetting factor $\lambda$ in the DFE is chosen as 0.999. In the PLL embedded in the DFE, the proportional tracking constant $K_{f_1}$ and the integral tracking constant $K_{f_2}$ are both set as 0.0002. The main parameters are listed in Table I.

Fig. 4 shows the selected CIR functions for the 4 transducer BPSK packet. As shown, the CIR functions exhibits fast fluctuation during the 2.5 s packet. Such fast fluctuating channels require frequent channel estimation. The other detrimental effect of the underwater acoustic channel is the fast phase fluctuation. In the MCC/DFE structure, it is treated by the Doppler tracking and correction. Fig. 5(a) shows the Doppler estimate at the four receiving elements for the 4 transducer BPSK packet. As shown, the Doppler estimates of different elements are largely correlated. The instantaneous Doppler estimates can be more than 4 Hz for the drifting source and receiver. When the Doppler correction has been made, the residual phase estimate is slowly variant as shown in Fig. 5(b).

The receiver performance is listed in Table II. For all the packets, the two receivers are able to track the channel. The maximum data rate is 32 kilobits/s achieved by the 4 transducer QPSK packet. The overall bit error rate (BER) of the packet is 0.06 for the receiver with SIC. SIC can improve the output SNR up to 3 dB. However, for the 4 transducer QPSK packet, the improvement is minimum (less than 1 dB for all symbol sequences). The demodulation order in SIC is preset according to the soft output SNR in the MCC/DEF receiver.

## V. CONCLUSION

In this paper, a MCC/DFE structure has been proposed for underwater acoustic MIMO channels. In order to overcome the difficulties introduced by the fast fluctuating channel, Doppler tracking and frequent channel estimation are performed. Then time reversal combining followed by a single channel DFE is used to demodulate individual symbol sequences transmitted by the multiple element source. SIC is also incorporated into the structure to improve the receiver performance. Using experimental data from MakaiEx, we have shown that the achievable data rate can be increased 2 to 4 times using the same bandwidth as single source systems.

## ACKNOWLEDGMENT

This research was supported by the Office of Naval Research (ONR) code 321OA. Authors wish to thank all the participants of MakaiEx.

## REFERENCES

[1] D. B. Kilfoyle and A. B. Baggeroer, "The state of the art in underwater acoustic telemetry," *IEEE J. Oceanic Eng.*, vol. 25, no. 1, pp. 4–27, Jan. 2000.

[2] I. E. Telatar, "Capacity of multi-antenna Gaussian channels," *European Trans. on Telecommunications*, vol. 10, no. 6, pp. 585–595, Nov. 1999.

[3] G. J. Foschini and M. J. Gans, "On limits of wireless communications in a fading environment when using multiple antennas," *Wireless Personal Commun.*, vol. 6, no. 3, pp. 311–355, 1998.

[4] V. Tarokh, N. Seshadri, and A. R. Calderbank, "Space-time codes for high data rate wireless communication: Performance criterion and code construction," *IEEE Trans. Info. Theory*, vol. 44, no. 2, pp. 744–765, Mar. 1998.

[5] M. Stojanovic, J. Catipovic, and J. G. Proakis, "Adaptive multichannel combining and equalization for underwater acoustic communications," *J. Acoust. Soc. Am.*, vol. 94, no. 3, pp. 1621–1631, Sept. 1993.

[6] M. Stojanovic, J. A. Catipovic, and J. G. Proakis, "Phase-coherent digital communications for underwater acoustic channels," *IEEE J. Oceanic Eng.*, vol. 19, no. 1, pp. 100–111, Jan. 1994.

[7] M. Stojanovic and Z. Zvonar, "Multichannel processing of broad-band multiuser communication signals in shallow water acoustic channel," *IEEE J. Oceanic Eng.*, vol. 21, no. 2, pp. 156–166, Apr. 1996.

[8] D. B. Kilfoyle, J. C. Preisig, and A. B. Baggeroer, "Spatial modulation experiments in the underwater acoustic channel," *IEEE J. Oceanic Eng.*, vol. 30, no. 2, pp. 406–178, Apr. 2005.

[9] S. Roy, T. M. Duman, V. McDonald, and J. G. Proakis, "High rate communication for underwater acoustic channels using multiple transmitters and space-time coding: Receiver structures and experimental results," *IEEE J. Oceanic Eng.*, vol. 32, no. 3, pp. 663–688, Jul. 2007.

[10] S. Roy, T. M. Duman, and V. McDonald, "Error rate improvement in underwater MIMO communications using sparse partial response equalization," *IEEE J. Oceanic Eng.*, submitted 2007.

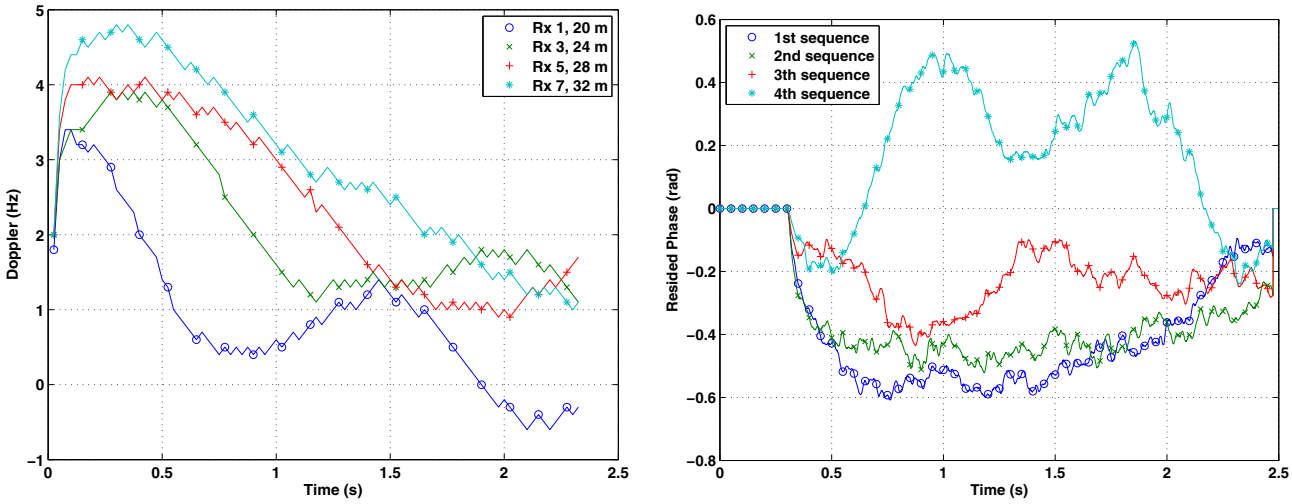


(a) (b)

Fig. 5. (a) The Doppler estimates at selected elements of the ACDS array. (b) The estimated residual phase for all the symbol sequences.

TABLE II
RECEIVER PERFORMANCE.

| Packet | Transducer | output SNR and BER | output SNR and BER with SIC | Demodulation order |
|---|---|---|---|---|
| BPSK, 1 Tx | 1 | $\rho = 14.2$ dB, BER=0/5568 | | |
| BPSK, 2 Tx | 1 | $\rho = 6.9$ dB, BER=15/5576 | $\rho = 9.6$ dB, BER=1/5576 | |
| | 2 | $\rho = 7.3$ dB, BER=1/5576 | $\rho = 7.3$ dB, BER=1/5576 | [2 1] |
| BPSK, 4 Tx | 1 | $\rho = 3.3$ dB, BER=194/5592 | $\rho = 5.4$ dB, BER=36/5592 | |
| | 2 | $\rho = 6.2$ dB, BER=19/5592 | $\rho = 6.2$ dB, BER=20/5592 | |
| | 3 | $\rho = 5.9$ dB, BER=29/5592 | $\rho = 8.0$ dB, BER=3/5592 | [2 3 1 4] |
| | 4 | $\rho = 1.8$ dB, BER=454/5592 | $\rho = 3.9$ dB, BER=138/5592 | |
| QPSK, 1 Tx | 1 | $\rho = 13.0$ dB, BER=0/5576 | | |
| QPSK, 2 Tx | 1 | $\rho = 5.6$ dB, BER=154/5592 | $\rho = 8.5$ dB, BER=34/5592 | |
| | 2 | $\rho = 6.0$ dB, BER=101/5592 | $\rho = 5.8$ dB, BER=105/5592 | [2 1] |
| QPSK, 4 Tx | 1 | $\rho = 0.9$ dB, BER=811/5596 | $\rho = 1.8$ dB, BER=601/5596 | |
| | 2 | $\rho = 4.1$ dB, BER=286/5596 | $\rho = 4.6$ dB, BER=245/5596 | |
| | 3 | $\rho = 6.5$ dB, BER=116/5596 | $\rho = 6.2$ dB, BER=122/5596 | [3 2 1 4] |
| | 4 | $\rho = 2.2$ dB, BER=520/5596 | $\rho = 2.5$ dB, BER=466/5596 | |


[11] H. C. Song, P. Roux, W. S. Hodgkiss, W. A. Kuperman, T. Akal, and M. Stevenson, "Multiple-input/multiple-output coherent time reversal communications in a shallow water acoustic channel," *IEEE J. Oceanic Eng.*, vol. 31, no. 1, pp. 170–178, Jan. 2006.

[12] H. C. Song, W. S. Hodgkiss, W. A. Kuperman, W. J. Higley, K. Raghukumar, and T. Akal, "Spatial diversity in passive time reversal communications," *J. Acoust. Soc. Am.*, vol. 120, no. 4, pp. 2067–2076, Apr. 2006.

[13] H. C. Song, W. S. Hodgkiss, W. A. Kuperman, T. Akal, and M. Stevenson, "Multiuser communications using passive time reversal," *IEEE J. Oceanic Eng.*, in press 2007.

[14] A. Song, M. Badiey, H.-C. Song, W. S. Hodgkiss, Michael Porter, and the KauaiEx Group, "Impact of ocean variability on coherent underwater acoustic communications during KauaiEx," *J. Acoust. Soc. Am.*, vol. 123, no. 2, pp. 856–865, Feb. 2008.

[15] M. B. Porter, "The Makai experiment: High frequency acoustics," in *Proc. Eighth European Conference on Underwater Acoustics*, Carvoeiro, Portugal, Jun. 2006.

[16] V. K. McDonald, P. Sullivan, T. M. Duman, S. Roy, J. G. Proakis, P. Hursky, and M. B. Porter, "Comprehensive MIMO testing in the 2005 Makai experiment," in *Proc. Eighth European Conference on Underwater Acoustics*, Carvoeiro, Portugal, Jun. 2006.

[17] J. G. Proakis, *Digital Communications*, McGraw-Hill, New York, 4th edition, 2000.

[18] C. C. Paige, "Fast numerically stable computations for generalized linear least squares problems," *SIAM J. NUMER. ANAL.*, vol. 16, no. 1, pp. 165–171, Feb. 1979.

[19] W. A. Kuperman, W. S. Hodgkiss, H. C. Song, P. Gerstoft, P. Roux, T. Akal, C. Ferla, and D. R. Jackson, "Ocean acoustic time reversal mirror," *Proc. Fourth European Conf. Underwater Acoustics*, pp. 493–498, 1998.

[20] G. F. Edelmann, T. Akal, W. S. Hodgkiss, S. Kim, W. A. Kuperman, and H. C. Song, "An initial demonstration of underwater acoustic communications using time reversal," *IEEE J. Oceanic Eng.*, vol. 31, no. 3, pp. 602–609, Jul. 2002.

[21] D. Rouseff, D. R. Jackson, W. L. J. Fox, C. D. Jones, J. A. Ritcey, and D. R. Dowling, "Underwater acosutic communication by passive-phase conjugation: Theory and experimental results," *IEEE J. Oceanic Eng.*, vol. 26, no. 4, pp. 821–831, Oct. 2001.

[22] T. C. Yang, "Temporal resolutions of time-reversal and passive-phase conjugation for underwater acoustic communications," *IEEE J. Oceanic Eng.*, vol. 28, no. 2, pp. 229–245, Apr. 2003.